Dependences of Brillouin frequency shift on strain and temperature in optical fibers doped with rare-earth ions

Yosuke Mizuno,[a] Neisei Hayashi, and Kentaro Nakamura
Precision and Intelligence Laboratory, Tokyo Institute of Technology, 4259 Nagatsuta-cho, Midori-ku, Yokohama 226-8503, Japan

(Received 13 May 2012; accepted 20 July 2012; published online 29 August 2012)

Brillouin scattering properties in rare-earth-doped fibers, including Nd^{3+}-doped, Tm^{3+}-doped, Sm^{3+}-doped, and Ho^{3+}/Tm^{3+} co-doped fibers, can potentially be controlled at high speed by pumping, but there has been no report on their detailed investigations. In this study, as the first step toward this goal, the Brillouin gain spectra (BGS) in such rare-earth-doped single-mode fibers are measured, for the first time, at 1.55 μm without pumping, and the Brillouin frequency shift (BFS) and its dependences on strain and temperature are investigated. Clear BGS was observed for the Nd^{3+}-doped and Tm^{3+}-doped fibers, but BGS was not detected for the Sm^{3+}-doped and Ho^{3+}/Tm^{3+} co-doped fibers probably because of their extremely high propagation losses at 1.55 μm and small Brillouin gain coefficients. The BFS of the Nd^{3+}-doped fiber was ~10.82 GHz, and its strain and temperature coefficients were 466 MHz/% and 0.726 MHz/K, respectively. As for the Tm^{3+}-doped fiber, the BFS was ~10.90 GHz, and its strain and temperature coefficients were 433 MHz/% and 0.903 MHz/K, respectively. These measurement results are compared with those of silica fibers. © *2012 American Institute of Physics*. [http://dx.doi.org/10.1063/1.4747926]

I. INTRODUCTION

For the past several decades, optical fibers doped with rare-earth ions, such as Er^{3+}, Nd^{3+}, Tm^{3+}, Sm^{3+}, Ho^{3+}, Yb^{3+}, and Pr^{3+}, have been extensively studied and applied to optical fiber amplifiers and fiber lasers.[1–3] In the meantime, Brillouin scattering in silica single-mode fibers (SMFs) has drawn considerable interest[4–7] and been applied to various devices and systems, such as lasers, tunable delay lines, phase conjugators, signal processors, slow light generators, optical storages, and strain/temperature sensors.[8–12] In order to improve their performance, Brillouin scattering properties in various non-silica fibers have been investigated, and some of them have already been practically applied. Such non-silica fibers include tellurite glass fibers,[13,14] chalcogenide glass fibers,[15,16] bismuth-oxide glass fibers,[14,17] photonic crystal fibers (PCFs),[18] polymethyl methacrylate (PMMA)-based polymer optical fibers (POFs), and perfluorinated graded-index (PFGI-) POFs.[19,20] Brillouin scattering in rare-earth-doped fibers has a big potential to offer high-speed signal controllability by pumping; and besides, with its amplification function, the measurement range of the Brillouin optical time-domain analysis or reflectometry (BOTDA/R)[8,11] will be elongated. Since its properties have not been investigated yet, detailed study on the Brillouin properties in rare-earth-doped fibers is the first step to exploit its potential in practical systems.

In this work, we measure the spontaneous Brillouin gain spectra (BGS) in four kinds of 2-m-long rare-earth-doped SMFs (Nd^{3+}-doped, Tm^{3+}-doped, Sm^{3+}-doped, and Ho^{3+}/Tm^{3+} co-doped fibers) at 1.55 μm without pumping, and investigate the Brillouin frequency shift (BFS) and its dependences on strain and temperature. While clear BGS was observed for the Nd^{3+}-doped and Tm^{3+}-doped fibers, no BGS was detected for the Sm^{3+}-doped and Ho^{3+}/Tm^{3+} co-doped fibers, which seems to be caused by their extremely high propagation losses at 1.55 μm and small Brillouin gain coefficients. The BFS of the Nd^{3+}-doped fiber was ~10.82 GHz, and its strain and temperature coefficients were 466 MHz/% and 0.726 MHz/K, respectively. As for the Tm^{3+}-doped fiber, the BFS was ~10.90 GHz, and its strain and temperature coefficients were 433 MHz/% and 0.903 MHz/K, respectively. We believe that these results will be an important archive in developing practical devices and systems based on Brillouin scattering in pumped rare-earth-doped fibers.

II. PRINCIPLE

When a light beam is injected into an optical fiber, it interacts with acoustic phonons and generates a backscattered light beam called the Stokes light.[5] This phenomenon is called Brillouin scattering, and the backscattered Stokes light spectrum is called the BGS. The center frequency of the BGS is known to be lower than that of the incident light, and the amount of this frequency downshift is called the BFS. In optical fibers, the BFS ν_B is given as

$$\nu_B = \frac{2 n v_A}{\lambda}, \tag{1}$$

where n is the refractive index, v_A is the acoustic velocity in the fiber, and λ is the wavelength of the incident light. One parameter for evaluating the Stokes power is the Brillouin threshold power P_{th}, which indicates the incident optical power required to induce the transition from spontaneous to stimulated scattering. P_{th} is given as[5]

[a]Author to whom correspondence should be addressed. Electronic mail: ymizuno@sonic.pi.titech.ac.jp.

TABLE I. BFS at room temperature and its strain and temperature coefficients in silica SMF, tellurite fibers, bismuth-oxide fibers, Ge-doped PCFs, and PFGI-POFs at 1550 nm.

Fiber	BFS (GHz)	Strain coefficient (MHz/%)	Temperature coefficient (MHz/K)
Silica SMF[a]	10.85	+580	+1.18
Tellurite[b]	7.95	−230	−1.14
Bismuth-oxide[c]	8.83	—	−0.88
Ge-doped PCF[d]	10.29	+409	+0.82
PFGI-POF[e]	2.83	−122	−4.09

[a]References 6 and 7.
[b]References 13 and 14.
[c]Reference 14.
[d]Reference 18.
[e]Reference 20.

$$P_{\mathrm{th}} = \frac{21\,A_{\mathrm{eff}}}{K\,g_{\mathrm{B}}\,L_{\mathrm{eff}}}, \tag{2}$$

where A_{eff} is the effective area, g_{B} is the Brillouin gain coefficient, K is the polarization parameter (= 0.667 when polarization state is not maintained), and L_{eff} is the effective length defined as

$$L_{\mathrm{eff}} = \frac{1 - e^{-\alpha L}}{\alpha}, \tag{3}$$

where α is the propagation loss and L is the fiber length. As P_{th} becomes lower, the Stokes power for the same incident power grows higher.

TABLE II. Physical properties of four FUTs used in experiments.

	Nd^{3+}	Tm^{3+}	Sm^{3+}	Ho^{3+}/Tm^{3+}
Product ID	Nd009	Tm134	Sm633	TH530
Length (m)	2	2	2	2
Core diameter (μm)	4	3	3	6
NA	0.18	0.16	0.14	0.18

Since one of the useful applications of Brillouin scattering is strain/temperature sensing, the BFS dependences on strain and temperature in various fibers have been investigated so far. Table I summarizes the BFS and its dependences on strain and temperature in silica SMFs,[6,7] tellurite fibers,[13,14] bismuth-oxide fibers,[14] Ge-doped PCFs (main peak only),[18] and PFGI-POFs.[20] Supposing that the wavelength of the incident light is 1550 nm and that n is not dependent on the wavelength, all the values in Table I have been recalculated using Eq. (1). As can be seen, the BFS and its strain and temperature dependences drastically change according to the fiber materials and structures.

III. EXPERIMENTAL SETUP

We employed as fibers under test (FUT) four kinds of rare-earth-doped SMFs manufactured by CorActive Inc.: Nd^{3+}-doped, Tm^{3+}-doped, Sm^{3+}-doped, and Ho^{3+}/Tm^{3+} co-doped fibers. Their lengths, core diameters, and numerical apertures (NAs), provided by the manufacturer, are summarized in Table II. One end of each FUT was spliced to a silica

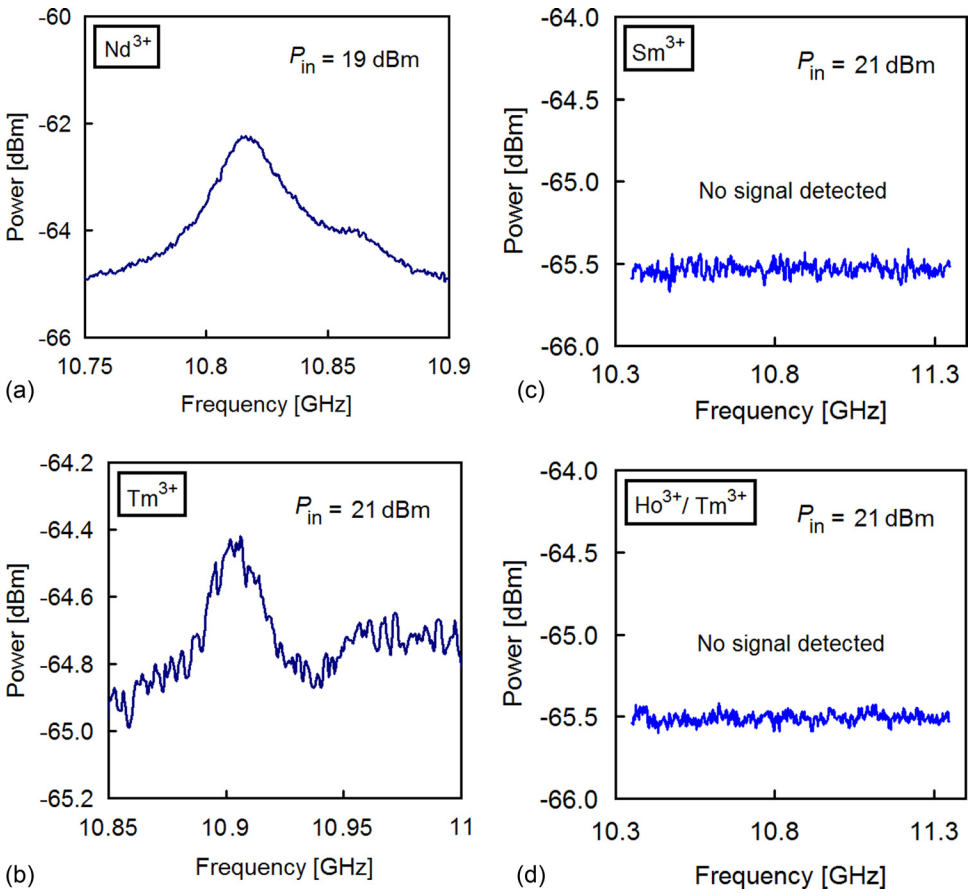

FIG. 1. Measured Brillouin gain spectra for (a) Nd^{3+}-doped, (b) Tm^{3+}-doped, (c) Sm^{3+}-doped, and (d) Ho^{3+}/Tm^{3+} co-doped fibers.

SMF connected to a circulator, and the other end was immersed into matching oil ($n = 1.46$) to suppress the Fresnel reflection.

The experimental setup for investigating the BFS dependences on strain and temperature in the FUTs was the same as that previously reported in Ref. 19, where self-heterodyne detection was used to observe the BGS with a high resolution. The wavelength of the light source was 1550 nm, and the polarization state was adjusted with a polarization controller (PC). The Brillouin signal generated in the silica SMF placed between the circulator and the FUTs was removed from the measurement results in the following procedure: (1) obtain the BGS when bending was applied to the region around the spliced point to induce considerable loss of >50 dB, (2) obtain the BGS after the bending was released, and (3) subtract the BGS obtained in (1) from that obtained in (2). Note that the bending-applied region was so short (<1 cm) that its influence on the measurement results was negligible. For each BGS measurement, 20-times averaging was performed.

IV. EXPERIMENTAL RESULTS

Figures 1(a)–1(d) show the measured BGS for the four FUTs. The incident optical power P_{in} was 19 dBm for the Nd^{3+}-doped fiber, and 21 dBm for the other fibers. Though distorted by the noise floor of the electrical spectrum analyzer (ESA), clear BGS was observed for the Nd^{3+}-doped and Tm^{3+}-doped fibers at ~10.82 GHz and at ~10.90 GHz, respectively, but no signal was detected for the Sm^{3+}-doped and Ho^{3+}/Tm^{3+} co-doped fibers both within and out of the range of Figs. 1(a) and 1(b).

In order to clarify the reason, the loss spectra of the four FUTs were measured using a white light source with a wavelength range of 350 to 1600 nm, as shown in Figs. 2(a)–2(d). We can see that the loss at 1550 nm is extremely high for the Sm^{3+}-doped and Ho^{3+}/Tm^{3+} co-doped fibers. Under the assumption that the loss in silica SMF and the spliced point is negligibly low (according to the manufacturer, splicing loss is as low as several dB for all the four fibers), the effective length L_{eff} at 1550 nm can be calculated to be 1.83, 1.33, 0.87, and 0.87 m for the Nd^{3+}-doped, Tm^{3+}-doped, Sm^{3+}-doped, and Ho^{3+}/Tm^{3+} co-doped fibers, respectively. (The loss of the Sm^{3+}-doped fiber is not exactly presented in Fig. 2(c), but the L_{eff} becomes almost constant when the loss is higher than 25 dB.) Although L_{eff} is relatively short for the Sm^{3+}-doped and Ho^{3+}/Tm^{3+} co-doped fibers, it does not appear to be the only cause for their weak Brillouin signals. Considering Eq. (2), since the effective areas of the four FUTs are in the same order judging from the core diameters given in Table II,[21] the main cause may be the difference in Brillouin gain coefficient, which needs to be further studied. It is worthwhile, however, to try to observe the Brillouin signal in the Sm^{3+}-doped and Ho^{3+}/Tm^{3+} co-doped fibers using a high-power light source at another wavelength such as 980 nm, which is one of the typical wavelengths used for pumping Er^{3+}-doped fibers.

Next, the BFS dependences on strain and temperature in the Nd^{3+}-doped and Tm^{3+}-doped fibers were investigated. The measured strain dependence of the BGS in the Nd^{3+}-

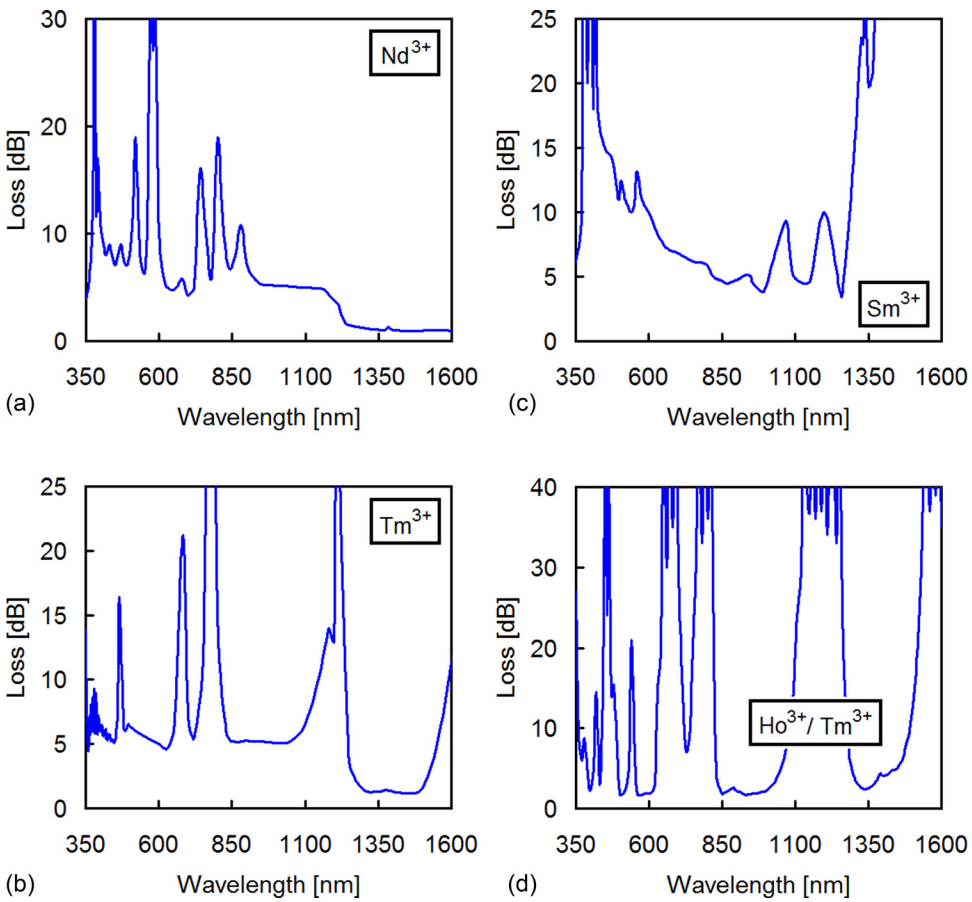

FIG. 2. Measured loss spectra of (a) Nd^{3+}-doped, (b) Tm^{3+}-doped, (c) Sm^{3+}-doped, and (d) Ho^{3+}/Tm^{3+} co-doped fibers. Note that the unit of the vertical axis is not dB/m but dB/(fiber length).

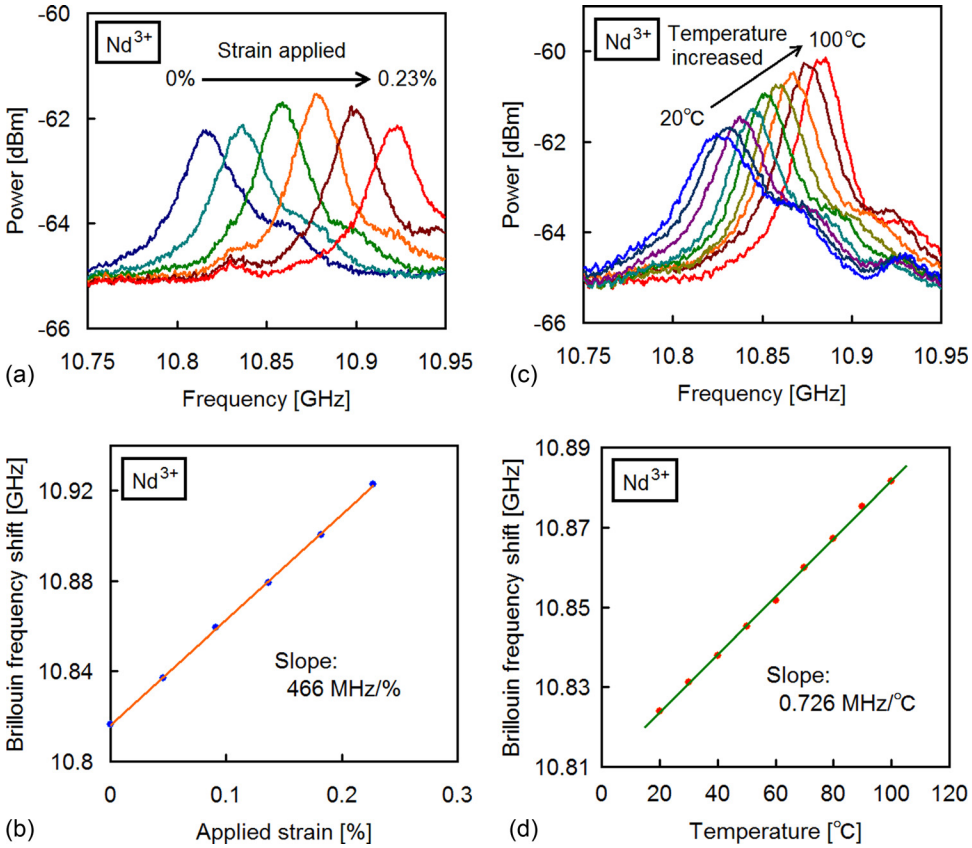

FIG. 3. Measured strain dependences of (a) BGS and (b) BFS, and temperature dependences of (c) BGS and (d) BFS in Nd^{3+}-doped fiber.

doped fiber is shown in Fig. 3(a). As the applied strain increased, the BGS shifted toward higher frequency. The change in Stokes power seems to be mainly due to the change in polarization state (note that the polarization state was not optimized for all the BGS measurements).[22] From Fig. 3(a), using a Lorentzian fitting of each BGS, the strain dependence of the BFS can be plotted as shown in Fig. 3(b). The strain dependence was almost linear with a coefficient

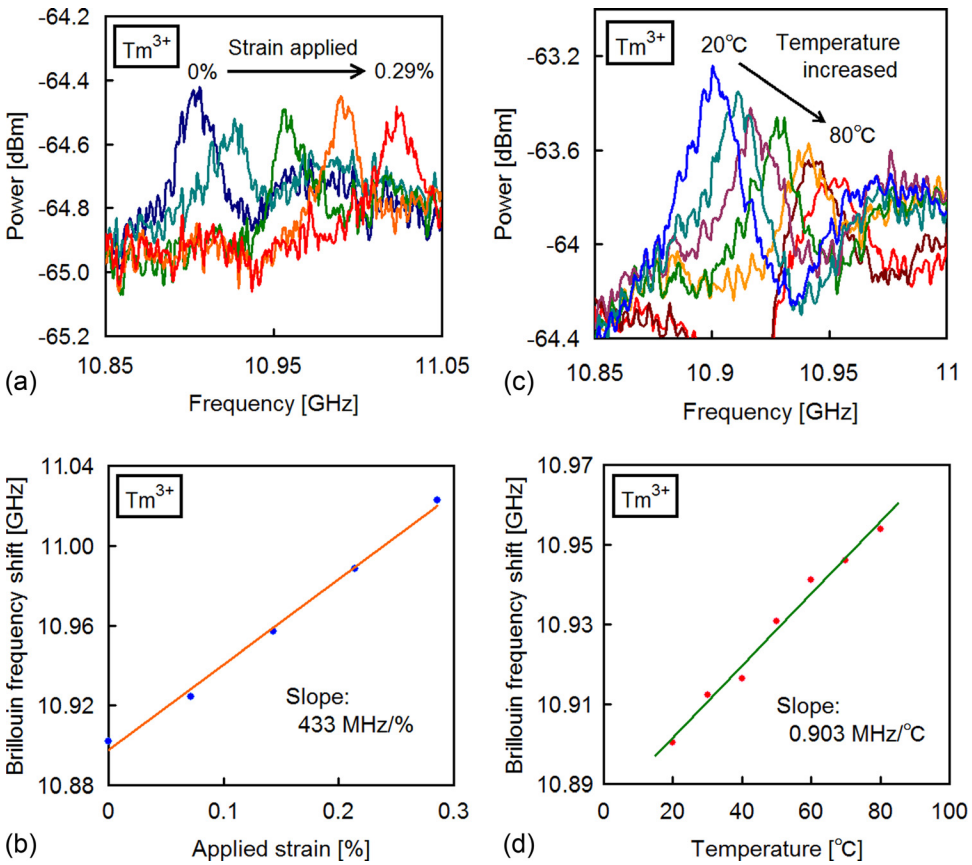

FIG. 4. Measured strain dependences of (a) BGS and (b) BFS, and temperature dependences of (c) BGS and (d) BFS in Tm^{3+}-doped fiber.

of 466 MHz/%. The BGS and BFS dependences on temperature were also investigated as shown in Figs. 3(c) and 3(d). The temperature coefficient of the BFS dependence was found to be 0.726 MHz/K.

In the same way, the BGS and BFS dependences on strain and temperature in the Tm^{3+}-doped fiber were investigated. The dependences on strain are shown in Figs. 4(a) and 4(b), and those on temperature are shown in Figs. 4(c) and 4(d). Although the Brillouin signal was so small that it was largely influenced by the change in polarization state as well as by the noise floor of the ESA, the BFS itself was properly measured. The strain and temperature coefficients of the BFS dependences in the Tm^{3+}-doped fiber were 433 MHz/% and 0.903 MHz/K, respectively. Thus, the strain and temperature coefficients of the BFS dependences were, in both the Nd^{3+}-doped and Tm^{3+}-doped fibers, lower than those of silica SMFs,[6,7] which indicates that these coefficients, along with the BFS itself, can be moderately controlled by adjusting the rare-earth doping concentration.

V. CONCLUSION

The BGS in four kinds of 2-m-long rare-earth-doped SMFs (Nd^{3+}-doped, Tm^{3+}-doped, Sm^{3+}-doped, and Ho^{3+}/Tm^{3+} co-doped fibers) was measured at 1.55 μm without pumping, and the BFS and its dependences on strain and temperature were investigated. The BFS at room temperature was ~10.82 GHz for the Nd^{3+}-doped fiber and ~10.90 GHz for the Tm^{3+}-doped fibers, but no BGS was detected for the Sm^{3+}-doped and Ho^{3+}/Tm^{3+} co-doped fibers probably due to their extremely high propagation losses at 1.55 μm and small Brillouin gain coefficients. The strain and temperature coefficients of the BFS dependences in the Nd^{3+}-doped fiber were 466 MHz/% and 0.726 MHz/K, respectively. As for the Tm^{3+}-doped fiber, the strain and temperature coefficients were 433 MHz/% and 0.903 MHz/K, respectively. We believe that these results will be an important archive in developing practical devices and systems based on pumped rare-earth-doped fibers with the high-speed controllability of their Brillouin signals.

ACKNOWLEDGMENTS

This work was supported by the Research Fellowships for Young Scientists from the Japan Society for the Promotion of Science (JSPS), and by research grants from the Foundation of Ando Laboratory and the Murata Science Foundation.

[1]M. J. F. Digonnet, *Rare-Earth-Doped Fiber Lasers and Amplifiers*, 2nd ed. (CRC, Boca Raton, 2001).
[2]P. Urquhart, "Review of rare earth doped fibre lasers and amplifiers," IEE Proc.-J: Optoelectron. **135**, 385–407 (1988).
[3]D. J. Richardson, J. Nilsson, and W. A. Clarkson, "High power fiber lasers: Current status and future perspectives," J. Opt. Soc. Am. B **27**, B63–B92 (2010).
[4]E. P. Ippen and R. H. Stolen, "Stimulated Brillouin scattering in optical fibers," Appl. Phys. Lett. **21**, 539–541 (1972).
[5]G. P. Agrawal, *Nonlinear Fiber Optics* (Academic, California, 1995).
[6]T. Horiguchi, T. Kurashima, and M. Tateda, "Tensile strain dependence of Brillouin frequency shift in silica optical fibers," IEEE Photon. Technol. Lett. **1**, 107–108 (1989).
[7]T. Kurashima, T. Horiguchi, and M. Tateda, "Thermal effects on the Brillouin frequency shift in jacketed optical silica fibers," Appl. Opt. **29**, 2219–2222 (1990).
[8]T. Horiguchi and M. Tateda, "BOTDA—Nondestructive measurement of single-mode optical fiber attenuation characteristics using Brillouin interaction: Theory," J. Lightwave Technol. **7**, 1170–1176 (1989).
[9]D. Garus, K. Krebber, F. Schliep, and T. Gogolla, "Distributed sensing technique based on Brillouin optical-fiber frequency-domain analysis," Opt. Lett. **21**, 1402–1404 (1996).
[10]K. Hotate and T. Hasegawa, "Measurement of Brillouin gain spectrum distribution along an optical fiber using a correlation-based technique—proposal, experiment, and simulation," IEICE Trans. Electron. **E83-C**, 405–412 (2000).
[11]T. Kurashima, T. Horiguchi, H. Izumita, S. Furukawa, and Y. Koyamada, "Brillouin optical-fiber time domain reflectometry," IEICE Trans. Commun. **E76-B**, 382–390 (1993).
[12]Y. Mizuno, W. Zou, Z. He, and K. Hotate, "Proposal of Brillouin optical correlation-domain reflectometry (BOCDR)," Opt. Express **16**, 12148–12153 (2008).
[13]Y. Mizuno, Z. He, and K. Hotate, "Distributed strain measurement using a tellurite glass fiber with Brillouin optical correlation-domain reflectometry," Opt. Commun. **283**, 2438–2441 (2010).
[14]Y. Mizuno, Z. He, and K. Hotate, "Dependence of the Brillouin frequency shift on temperature in a tellurite glass fiber and a bismuth-oxide highly nonlinear fiber," Appl. Phys. Express **2**, 112402 (2009).
[15]K. S. Abedin, "Observation of strong stimulated Brillouin scattering in single-mode As_2Se_3 chalcogenide fiber," Opt. Express **13**, 10266–10271 (2005).
[16]K. Y. Song, K. S. Abedin, K. Hotate, M. G. Herráez, and L. Thévenaz, "Highly efficient Brillouin slow and fast light using As_2Se_3 chalcogenide fiber," Opt. Express **14**, 5860–5865 (2006).
[17]J. H. Lee, T. Tanemura, K. Kikuchi, T. Nagashima, T. Hasegawa, S. Ohara, and N. Sugimoto, "Experimental comparison of a Kerr nonlinearity figure of merit including the stimulated Brillouin scattering threshold for state-of-the-art nonlinear optical fibers," Opt. Lett. **30**, 1698–1700 (2005).
[18]L. Zou, X. Bao, S. Afshar, and L. Chen, "Dependence of the Brillouin frequency shift on strain and temperature in a photonic crystal fiber," Opt. Lett. **29**, 1485–1487 (2004).
[19]Y. Mizuno and K. Nakamura, "Experimental study of Brillouin scattering in perfluorinated polymer optical fiber at telecommunication wavelength," Appl. Phys. Lett. **97**, 021103 (2010).
[20]Y. Mizuno and K. Nakamura, "Potential of Brillouin scattering in polymer optical fiber for strain-insensitive high-accuracy temperature sensing," Opt. Lett. **35**, 3985–3987 (2010).
[21]D. Marcuse, "Loss analysis of single-mode fiber splices," The Bell Syst. Tech. J. **56**, 703–718 (1977).
[22]Y. Mizuno, Z. He, and K. Hotate, "Stable entire-length measurement of fiber strain distribution by Brillouin optical correlation-domain reflectometry with polarization scrambling and noise-floor compensation," Appl. Phys. Express **2**, 062403 (2009).